

Super Planckian Thermal Radiation Emitted From a Nano-Filament of Photonic Crystal: A Direct Imaging Study

Mei-Li Hsieh,¹ Shawn-Yu Lin ¹, *Member, IEEE*, Sajeev John,²
James A. Bur,¹ Xuanjie Wang,³ Shankar Narayanan,³
and Ting-Shan Luk⁴

¹Department of Physics, Applied Physics and Astronomy, Rensselaer Polytechnic Institute, Troy, NY 12180 USA

²Department of Physics, University of Toronto, Toronto, ON M5S 1A7, Canada

³Department of Mechanical, Aerospace and Nuclear Engineering, Rensselaer Polytechnic Institute, Troy, NY 12180 USA

⁴Sandia National Laboratory, Albuquerque, NM 87185 USA

DOI:10.1109/JPHOT.2019.2948995

This work is licensed under a Creative Commons Attribution 4.0 License. For more information, see <https://creativecommons.org/licenses/by/4.0/>

Manuscript received September 15, 2019; revised October 16, 2019; accepted October 18, 2019. Date of publication October 22, 2019; date of current version November 26, 2019. The work of S.-Y. Lin was supported by the National Science Foundation under Award ECCS-1840673-NOA (device fabrication and characterization). The work of S. John was supported by the DOE Office of Science under Award DE-FG02-06ER46347 (theoretical modeling). Corresponding author: Shawn-Yu Lin (e-mail: sylin@rpi.edu).

Abstract: In this paper, we report a direct imaging of narrow-band super Planckian thermal radiation in the far field, emitted from a resonant-cavity/tungsten photonic crystal (cavity/W-PC). A spectroscopic study of the cavity/W-PC shows a distinct resonant peak at $\lambda \sim 1.7 \mu\text{m}$. Furthermore, an infrared CCD camera was used to record radiation image of the cavity/W-PC and a carbon-nanotube (CNT) black reference at $\lambda \sim 1.7 \mu\text{m}$ emitted from the same sample. The recorded image displays a higher brightness emitted from the cavity/W-PC region than from the blackbody region for all temperatures tested, $T = 530\text{--}650 \text{ K}$. This observation is in sharp contrast to the common understanding of equilibrium thermal radiation, namely, a blackbody has a unit absorptance, a unity emittance and should emit the strongest radiation. Since the image was taken from the same sample and the temperature difference across the W-PC/ CNT boundary is less than 0.1 K, the observed image contrast gives a truly convincing evidence of super Planckian behavior in our sample. The discovery of a super-intense, narrow band radiation from a heated W-PC could open up a new door for realizing narrow band infrared emitters. The W-PC filament could also be very useful for efficient energy applications such as thermo-photovoltaics, waste heat recycling and radiative cooling.

Index Terms: Nano-photonics, photonic crystals, novel photon sources, photonic materials and engineered photonic structures.

Blackbody radiation is a fundamental property of matter at finite temperatures and its radiation spectrum was first derived by M. Planck in 1900 [1]. In his formulation, the concept of photon was introduced and the Bose-Einstein statistics used to describe equilibrium distribution of the emitted photons. Planck's blackbody radiation law also sets the upper limit of radiation intensity at equilibrium in the far field (the blackbody limit). In the absence of thermal equilibrium, deviations from the Planck's distribution may occur [2], [3]. An interesting set of earlier experiments has revealed that certain photonic-crystal (PC) structures when driven out of equilibrium can exhibit

significant deviation from the blackbody [4]–[6]. A further spectroscopic study on resonant cavity/photonic crystal samples suggested that radiation intensity at the resonant peaks may exceed those of conventional blackbody under similar experimental conditions [7]. The finding is striking, and if it is indeed independently verified, the realization of a super-intense narrow band near-infrared radiation could impact a wide variety of energy applications, such as thermo-photovoltaics, waste heat recycling and radiative cooling/ heating. This new class of narrow band infrared source could also be useful for infrared imaging and chemical spectroscopy purposes.

In this paper, we report an imaging along with a spectroscopic study of far-field super-Planckian thermal radiation at optical wavelengths, i.e., at $\lambda = 1.7 \mu\text{m}$. The imaging method combines an infrared CCD (charge couple device) camera and an imaging telescope to record light emission from a thermally heated sample. A filter with an optical passband of $\lambda = 1600\text{--}1800 \text{ nm}$ was used to ensure that only radiation in the narrow band spectral range was detected by the CCD camera. About half of the PC sample was coated with a thin-layer of black VA-CNT (vertically aligned carbon nano-tube) having an $A = 99.9\text{--}99.98\%$ absorptance, which provides for the blackbody reference. Thermal flow analysis (COMSOL Multiphysics 5.2a) indicates that sample's surface temperature in areas with and without CNT coating is uniform to within 5 K across the sample. Under this configuration, the imaging measurement was conducted and the corresponding narrow-band infrared images recorded for a series of sample's surface temperatures $T = 530\text{--}650 \text{ K}$. It was found that the recorded image has a higher brightness from the cavity/W-PC region than from the black CNT region for all temperatures tested. This is in sharp contrast to the conventional understanding of equilibrium radiation that a blackbody has a unity absorptance and emittance and, therefore, should give the brightest radiative power. A further quantitative analysis of the image shows that the PC radiation intensity is 3.7~5 times higher than that of a blackbody emitter at 650 K, providing a direct evidence of super Planckian thermal radiation at $\lambda \sim 1.7 \mu\text{m}$ in the far-field.

Fig. 1(a) shows a drawing of standard blackbody radiation spectra at $T = 800 \text{ K}$, 900 K , 1000 K (the red, green and blue curves) and also a schematic of a narrow-band radiation that is beyond the blackbody limit (the red, green and blue bars), respectively. Fig. 1(b) shows a schematic of our resonant cavity/tungsten photonic crystal (W-PC) sample. The W-PC is mounted on top of an electrical driven heater by $\sim 300 \mu\text{m}$ thick blackbody paint [8]. The W-PC/ heater assembly is then mounted on a one-inch long ceramic post to dewar pumped to $10^{-6}\text{--}10^{-7}$ Torr to eliminate thermal convection loss. An infrared NaCl window is used for optical transmission purpose. About half of the sample's top surface is covered with a layer of VA-CNT, having a total absorptance of $A = 99.9\text{--}99.98\%$ [9], [10]. The VA-CNT material was grown separately on a Ni-seeded silicon substrate. It was then peeled off from the silicon substrate and transferred and glued to the PC-sample by thermally conductive blackbody paint. The VA-CNT has a layer thickness of $400 \mu\text{m}$ and a thermal conductivity of $\kappa = 2000\text{--}6000 \text{ Watts/m-K}$ [11]. According to our COMSOL model calculation, the temperature difference between the top and the bottom CNT surfaces is less than 0.1 K due to its high thermal conductivity. The computational modeling conducted in this study took into account the thermophysical properties and geometry of each layer to predict the temperature accurately. In this regard, we also validated our simulations using multiple experiments that recorded the steady-state temperatures of our sample's top surface. The predicted and the calculated values show good agreement for multiple cases. Fig. 1(c) shows a schematic of the top view (x-y plane) of the sample, where its right-hand side is covered with VA-CNT material (the black color region). Fig. 1(d) shows the computed temperature profile of the sample's top surface at a heater input power of $P = 5 \text{ Watts}$. The center region is about 5 K hotter than the edges, which is the maximum temperature variation across the sample. The slight oval-shape of the constant temperature contour is due to the slight rectangular shape of the heater geometry. Fig. 1(e) shows the computed temperature distribution across the sample's top surface (along the red dashed line) for a series of heater's input power $P = 4, 5, 6$ and 7 Watts . The temperature variation across the sample is 3, 4, 5, and 5 K for $P = 4, 5, 6$ and 7 Watts , respectively. Note also that there is no observable temperature difference ($<0.1 \text{ K}$) across the boundary between W-PC and VA-CNT regions. The insert of Fig. 1(e) shows the computed 3D temperature profile of the sample at $P = 5 \text{ Watts}$. The heating filament is found to be $\sim 40 \text{ K}$ hotter than the sample's surface temperature.

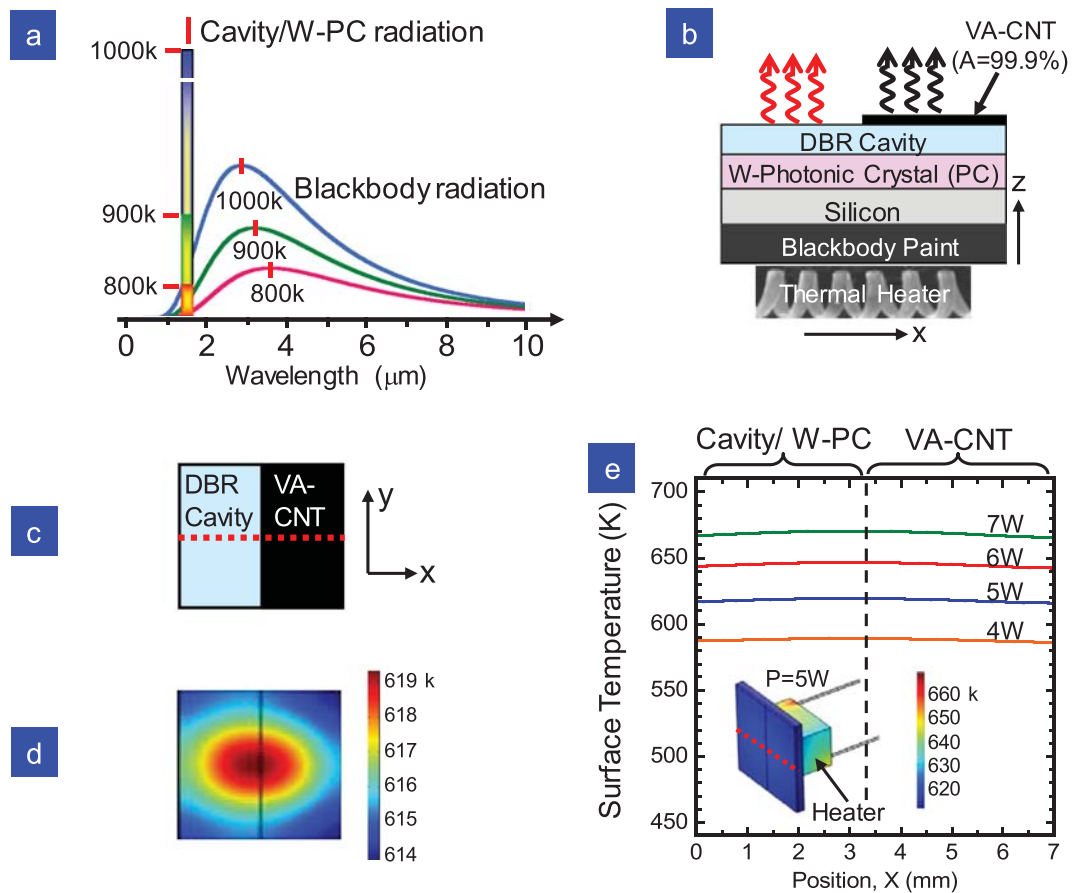


Fig. 1. (a) A schematic drawing, illustrating the narrow band radiation spectrum of a resonant-cavity/tungsten photonic crystal filament (W-PC) at $\lambda \sim 1.7 \mu\text{m}$ and the standard, broad blackbody radiation spectra at $T = 800$ K, 900 K, and 1000 K, respectively. (b) A schematic of the cross section structure of our cavity/W-PC sample. The sample is heated by a thermal heater. About half of the sample's top surface is covered with a layer of VA-CNT (vertically-aligned carbon nanotube), having a total reflectance of $A = 99.9 \sim 99.98\%$. (c) A schematic of the top surface of the W-PC sample, having half of its surface area covered by a VA-CNT material. (d) shows the computed temperature profile of the sample's top surface at a heater input power of $P = 5$ Watts. (e) The temperature distribution across the sample's top surface for a range of heater's input power, $P = 4, 5, 6, 6$ Watts. The inset shows a 3D temperature profile of the sample with a heater. The temperature scale bar is color-coded.

Accordingly, this slightly higher temperature might contribute to a weak non-equilibrium pumping for an enhanced W-PC radiation.

The sample used in this experiment consists of a micro-cavity fabricated on top of a 3D W-PC on a four-inch silicon wafer. The detail structure has been described earlier [7]. Here, we only give a brief account of it. The micro-cavity is formed by a SiO_2 layer of thickness $t_{\text{cav}} = 554$ nm sandwiched on both sides by SiO_2/Si Distributed Bragg Reflector (DBR) mirrors. The thicknesses of the SiO_2 and Si are $t_{\text{oxide}} = 275$ and $t_{\text{Si}} = 120$ nm, respectively. The 3D W-PC has diamond lattice symmetry and consists of six layers of alternating one-dimensional tungsten-rods [12]–[14]. The 1D tungsten-rods have a height of $h = 0.6 \mu\text{m}$, a rod width of $w = 0.5 \mu\text{m}$ and a rod-to-rod spacing of $a = 1.5 \mu\text{m}$. The PC-cavity sample area is $\sim 7 \times 7 \text{ mm}^2$ and the silicon substrate has a thickness of $\sim 300 \mu\text{m}$.

We will first conduct spectroscopic study of the radiation spectrum of the heated cavity/W-PC. The purpose is to identify its radiation peak that corresponds to the fundamental resonant wavelength of the cavity/W-PC sample. This spectroscopic result will then allow us to perform imaging study of the

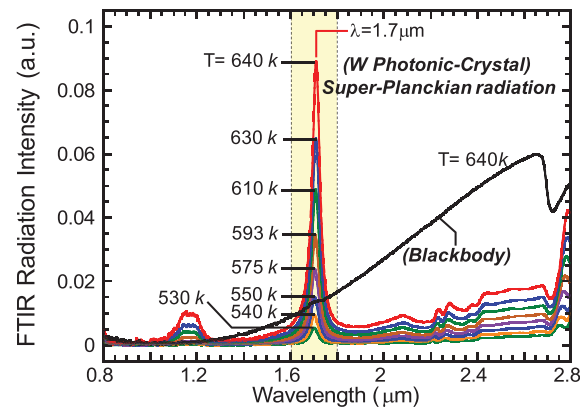


Fig. 2. Thermal radiation spectra of our resonant cavity/ W-PC sample, taken at a series of lattice temperatures, $T = 530\text{--}640$ K. The VA-CNT radiation is also shown as a blackbody reference at 640 K. The W-PC sample exhibits a distinctly sharp radiation peak at $\lambda = 1600\text{--}1800$ nm (indicated as the yellow region), far beyond the standard blackbody intensity.

cavity/W-PC radiation peak at a narrow band. Very importantly, in the current study, spectroscopic testing of both the cavity/W-PC and blackbody reference was performed on the same sample and the same heating conditions. This is done by coating a small fraction of the sample ($\sim 30\%$) with a black VA-CNT material and subsequently performing measurements on and off the VA-CNT area. This method is new and is to eliminate measurement uncertainty when taking the test samples in and out of the vacuum chamber. The method also ensures that both the cavity/ W-PC and VA-CNT radiation data were taken from the same sample, with a surface temperature uniform to within 5 K. While a similar spectroscopic study was reported earlier [7], its blackbody reference was obtained from a separately coated sample and, hence, might be less accurate or convincing.

Fig. 2 shows results of the measured radiation spectra of the heated cavity/W-PC sample at a series of sample's surface temperatures $T = 530\text{--}640$ K. Also shown is a blackbody spectrum taken at 640 K. The cavity/W-PC radiation spectrum shows a distinct peak at $\lambda \sim 1.7 \mu\text{m}$ with a FWHM (full-width-half-maximum) of $\Delta\lambda \sim 40$ nm. This narrow line width is more compatible to that of a typical Ga1nN/GaN light-emitting-diode of $\Delta\lambda \sim 30$ nm at $\lambda \sim 460$ nm [15] than that of a standard blackbody radiator of $\Delta\lambda \sim 5.5 \mu\text{m}$ at 640 K. Contrary to Wien's displacement Law [16], the wavelength of peak radiation is nearly independent of sample's surface temperature and pinned at $\lambda \sim 1.7 \mu\text{m}$. At the same time, its peak radiation intensity at 640 K is ~ 7 times higher than that of the blackbody also at 640 K. Given the method used and uniformity of sample's surface temperature, this data provides a convincing evidence of super-Planckian thermal radiation being emitted from our cavity/W-PC sample at $\lambda \sim 1.7 \mu\text{m}$ in the far field.

It may be argued that the 7-time radiation enhancement is due to a hotter sample's surface T in the cavity/W-PC region. Or, the cavity/W-PC radiation enhancement is due to leakage of light from a hotter heating filament underneath the sample structure. Both are valid considerations, but they are not likely to occur in our device. The reason is as follows. First, an FTIR (Fourier-transform-Infrared-Spectrometer) study shows that there is negligible transmission ($<0.5\%$) of light at $\lambda \sim 1.7 \mu\text{m}$ through our cavity/W-PC sample. Therefore, leakage of light from the heating filament should not be significant. Also, in our testing setup, the radiation from our sample is detected through double apertures of 2 mm in diameter that are separated by 3 cm apart. The potential leakage of higher- T radiation from the chamber wall into the FTIR system would be off the angle and is, therefore, negligible. Second, if the cavity/W-PC region is to have a hotter sample's surface T , it would have to be 110 K hotter than the CNT-region to account for the 7-time enhancement. A brief quantitative analysis based on Planck's blackbody radiation law [1], [16] is shown below. When the emitted photon energy ($\hbar\omega$) is much larger than the thermal energy ($\hbar\omega \gg k_b T$), the Bose-Einstein distribution function becomes approximately the Boltzmann distribution function, $1/(e^{\hbar\omega/k_b T} + 1) \cong e^{-\hbar\omega/k_b T}$. The temperature dependence of blackbody radiation intensity at a fixed

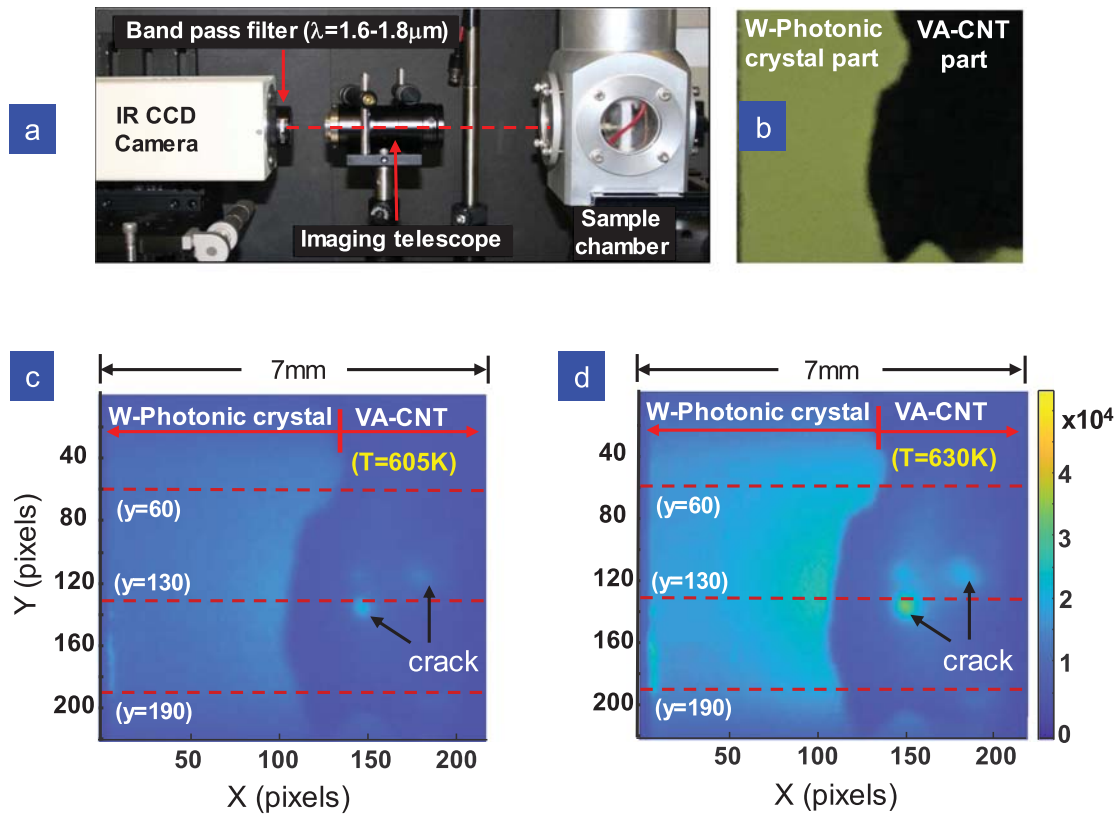


Fig. 3. (a) A photo of our near-infrared imaging set up. Thermal radiation is emitted from a heated W-PC sample. An imaging telescope is used to project the emitted radiation onto a near-infrared CCD camera ($\lambda = 0.85 - 2.2 \mu\text{m}$). The bandpass filter is to ensure that only that radiation in the $\lambda = 1600 - 1800 \text{ nm}$ spectral range is recorded. (b) A photo of the sample taken by a camera at visible wavelength and at room temperature. The W-PC sample is covered with a VA-CNT (the black region) on the right hand side of it. (c) and (d) Infrared images of the W-PC sample shown in Fig. 3(b) heated to $T = 605$ and 630 K , respectively. The color-coded scale bar is also shown. The VA-CNT has an absorptance of $99.9\sim 99.98\%$, which serves as the blackbody reference. The radiation from the W-PC area is brighter than that from the VA-CNT area.

wavelength is then given by the Boltzmann factor. Therefore, the ratio of the distribution function at two different temperatures (T_1 and T_2) becomes $\eta = (e^{-\hbar\omega/k_b T_2}) / (e^{-\hbar\omega/k_b T_1})$. Here, we assume that the enhancement factor η is due entirely to the temperature difference of the emitter. In our case, when $\lambda \sim 1.7 \mu\text{m}$, $T_1 = 640 \text{ K}$ and $\eta = 7$, we found $T_2 = 750 \text{ K}$. In other words, the temperature in the W-PC region would have to be 110 K hotter than the VA-CNT region to account for the observed W-PC radiation enhancement. This is not likely to occur as sample's surface temperature is uniform to within 5 K . And, also, the hottest T of the system is the heating filament, which is $\sim 40 \text{ K}$ hotter than the samples' top surface.

An independent and even more direct verification of the Super-Planckian radiation is performed using a near-infrared (IR) imaging method. Fig. 3(a) shows a photo of the infrared imaging setup. Thermal radiation is emitted from a heated cavity/W-PC sample of $\sim 7 \times 7 \text{ mm}^2$ in size, which is placed inside a vacuum sample chamber. An imaging telescope is used to project the emitted radiation onto a near-IR CCD camera, with a spectral response $\lambda = 0.85 - 2.2 \mu\text{m}$. The bandpass filter is to ensure that only the narrow band radiation in the $\lambda = 1600 \text{ nm} - 1800 \text{ nm}$ range (the light yellow region in Fig. 2) is detected. Fig. 3(b) shows a photo of the cavity/W-PC sample, which is taken by a camera at visible wavelength and at room temperature. About half of the W-PC sample is covered with a VA-CNT (the black region) piece on the right hand side of it. The VA-CNT has a total absorptance of $99.9\sim 99.98\%$ in the visible and infrared wavelengths [9], [10]. The zigzag

boundary of the VA-CNT piece is due to a non-ideal peeling off procedure of the VA-CNT layer from the silicon substrate where it was originally grown. There are also a few cracks within the VA-CNT piece, due perhaps also to the peeling-off practice.

Fig. 3(c) and 3(d) shows a recorded raw data of the near-IR image of a heated cavity/W-PC sample at 605 and 630 K, respectively. The grey-level of the image intensity is color coded for clarity and a corresponding scale bar is also shown. As expected, when samples' surface temperature is increased from 605 K to 630 K, the corresponding IR image becomes brighter. Moreover, both images display several common features that are worth mentioning. **First**, it is observed that the overall radiation from the cavity/W-PC region is brighter than that from the VA-CNT region. The center region of the sample is slightly brighter due partly to a slightly hotter temperature profile as illustrated in Fig. 1(d). **Secondly**, there is a clear contrast of brightness across the cavity/W-PC and the VA-CNT (PC/CNT) boundary. Given that temperature uniformity across the sample and the PC/CNT boundary is better than 5 K and 0.1 K, respectively, these images represent a truly accurate comparison of cavity/W-PC and blackbody radiation intensity in the far-field. **Thirdly**, at and near the crack regions, the radiation is distinctly brighter than its surrounding VA-CNT region. There is also certain degree of light spreading around the crack. It is worth noting that the crack exposes the underneath cavity/W-PC radiation, which is again brighter than that from the surrounding VA-CNT material.

To provide a quantitative analysis of the CCD image shown in Fig. 3(c) and 3(d), we record the image's grey-level intensity along a line across the sample. Specifically, a total of three line scans along the x-direction was recorded at $y = 60, 130, 190$ pixels (the red dashed line in Fig. 3(c) and 3(d)). The hope was to observe a rapid change of radiation intensity across the PC/CNT boundary. The same analysis was also repeated for CCD images taken at a series of sample's surface temperatures, $T = 530\text{--}650$ K.

Fig. 4(a) shows the CCD intensity as a function of the x- position along the red dashed line at $y = 60$ pixels. The CCD image has a background intensity of $I \sim 0.5 \times 10^4$ and a noise level of $\Delta I \sim 0.1 \times 10^4$. At $T = 650$ K, the CCD intensity increases slightly from $x = 10$ to ~ 130 , drops rapidly at the PC/CNT boundary at $x \sim 135$ and then decreases to the background level near the sample edge for $x > 200$. This rapid drop of the CCD intensity across the PC/CNT boundary offers a quantitative comparison of the radiation intensity between that emitted from the cavity/W-PC and the VA-CNT. Given the temperature difference across the PC/CNT boundary (the vertical red dashed line) is less than 0.1 K, this rapid intensity drop across the boundary is a truly convincing evidence of super-Planckian radiation been emitted from the cavity/W-PC into the far field. Furthermore, one may define an intensity enhancement factor as: $\eta \equiv \frac{(PC \text{ Intensity} - background)}{(VA \text{ CNT Intensity} - background)}$. We found $\eta = 3.7$ at $T = 650$ K. Again, it may be argued that the 3.7-time cavity/W-PC radiation enhancement is due to a hotter sample's surface T in the cavity/W-PC region. If this is indeed the case, the cavity/W-PC region would have to be ~ 72 K hotter than the CNT-region [17]. This is unlikely as sample's surface temperature is uniform to within 5 K across the sample. Further analysis of the data in Fig. 4(a) for images taken at lower temperatures gives an even higher enhancement factor. When sample's surface temperature is decreased from 630, 620, 605, 585 to 575 K, the enhancement factor is found to be increased from $\eta = 3.9, 5.3, 5.8, 7.3$ to 9.5, respectively.

Fig. 4(b) show the line scan result along $y = 130$. In this case, the CCD intensity increases slightly from $x = 10\text{--}60$ and more rapidly from $x = 60\text{--}100$. At $x \sim 110$, a rapid intensity drop across the PC/CNT boundary was observed. The rapid drop at $x = 110$ is again a confirmation of super-Planckian radiation been emitted from the cavity/W-PC region. The enhancement factor is found to be $\eta = 4.5, 5.3, 6, 7.5, 7.8$ and 10 at $T = 650, 630, 620, 605, 585$ and 575 K, respectively. Interestingly, even though the crack was introduced un-intentionally in the VA-CNT region, it allows the leakage of a much stronger W-PC radiation within an otherwise weaker VA-CNT radiation region. For example, a small crack exists at $x \sim 150$, where a strong CCD intensity peak was observed. The peak has a slightly stronger intensity (CCD intensity = 3.4×10^4) than that in the W-PC region (CCD intensity = 3×10^4) due perhaps to a slight area concentration of radiation through the crack. The leakage of light also shows a significant spreading around the crack over

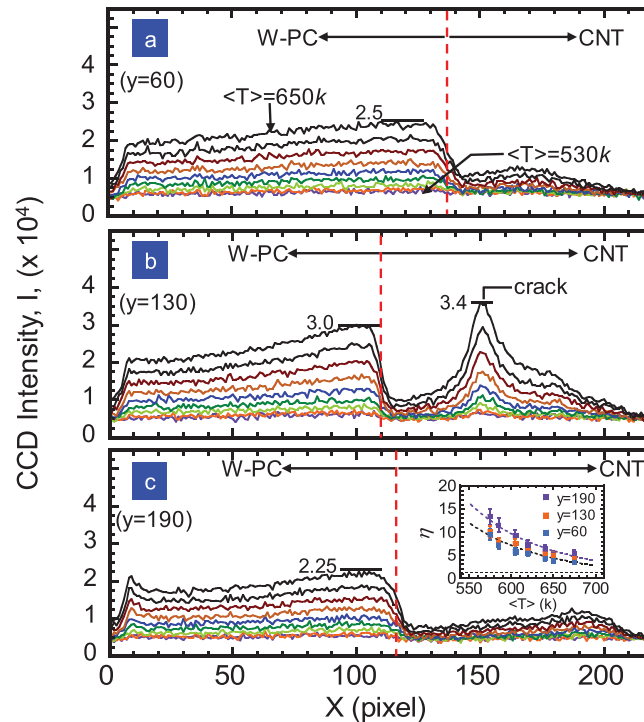


Fig. 4. (a) The CCD image intensity vs. x -position along the red dashed line at $y = 60$ (see Fig. 3c) for a range of temperatures, $T = 530$ – 650 K. The CCD intensity has a background level of $I \sim 0.5 \times 10^4$. At $T = 650$ K, the intensity increases slightly from $x = 10$ to $x \sim 130$, drops abruptly at $x = 130$ – 150 and decreases to the background level near the sample edge at $x \geq 200$. (b) The CCD image intensity vs. x -position along the red dashed line at $y = 130$. Here, the rapid drop in intensity occurs at $x \sim 100$ – 110 for all temperatures. The intensity peak at $x \sim 150$ is due to a small crack in the VA-CNT coating layer. (c) The CCD image intensity vs. x -position along the red dashed line at $y = 190$. Here, the rapid drop in intensity occurs at $x \sim 110$ – 120 also for all temperatures tested.

about 50 pixels' spatial range. At present, the reason for area concentration and spatial spreading is not known. Similarly, Fig. 4(c) shows the line scan results along $y = 190$. This time, the rapid drop in CCD intensity occurs at $x \sim 115$ and the corresponding enhancement factor is $\eta = 5, 6, 7.3, 9.2, 11.5,$ and 13.3 at $T = 650, 630, 620, 605, 585$ and 575 K, respectively. The overall weaker CCD intensity for the $y = 190$ vs the $y = 130$ data may be due to the fact that the radiation is taken from the sample's far edge where sample's temperature is lower.

In the inset of Fig. 4(c), we summarize the T -dependence of η at $\lambda = 1.7 \mu\text{m}$ for all three line scans at $Y = 60, 130,$ and 190 , respectively. The experimental accuracy of η is estimated to be 10% due mainly to the background noise of the grey-level signal. We found that η decreases rapidly as T is increased and has an empirical $(T)^{-6}$ dependence. The purple and black dashed lines are fitting curves to the data for $Y = 190$ and $Y = 130/60$ scans, respectively. The temperature dependence of the enhancement factor at 1.7 microns is likely due to metallic losses in the tungsten (arising from the electronic scattering rate) that increase with temperature, as modeled in reference-2. In this model, light output intensity is diminished by temperature-dependent resistivity in the metal.

In summary, we report a direct probing of narrow band super-Planckian thermal radiation emitted from a cavity/W-PC filament in the far field. Two independent testing were performed, one is a frequency-domain spectroscopy and the other a spatial-domain infrared imaging method. The spectroscopic comparison of the cavity/W-PC and black reference was done on the same sample and the same heating conditions. The method ensures that the comparison of radiation intensity is accurate and thus the observed super Planckian behavior is conclusive. Furthermore, an infrared imaging was done for a cavity/W-PC sample at $T = 530$ – 650 K, having half of it covered with a black CNT material. At $T = 650$ k, the infrared image shows (3.7-5) times brighter intensity emitted

from the cavity/W-PC than that from a standard blackbody. This discovery is in sharp contrast to the conventional knowledge that a blackbody has a unity absorptance, a unity emittance and should emit the strongest radiation at any given temperature. Since the temperature difference across the PC/CNT boundary is less than 0.1 K, the observed image contrast gives a truly convincing evidence of super Planckian behavior in our cavity/W-PC sample. The observed super-Planckian radiation may originate from the existence of non-linear Bloch waves and the excitation of localized surface plasmons throughout the W-PC interior [2], [18]–[20]. Finally, the discovery of a narrow-band super Planckian radiation in the far field has important technological consequences in area such as highly efficient thermo photovoltaics [5], efficient optical emitter driven by waste heat and also passive radiative cooling [21]. The demonstrated nano-filament of W-PC is a new type of super-intense infrared emitter. It represents a new class of narrow band infrared source that could be useful for IR imaging, IR tracking and also chemical spectroscopy.

Acknowledgment

S.Y. Lin would like to thank X.-M. Li for making useful suggestions on thermal flow analysis.

References

- [1] M. Planck, *The Theory of Heat Radiation*, New York, NY, USA, Dover, 1959.
- [2] A. Kaso and S. John, "Nonlinear bloch waves in metallic photonic band-gap filaments," *Phys. Rev. A*, vol. 76, 2007, Art. no. 53838.
- [3] W. W. Chow, "Theory of emission from an active photonic lattice," *Phys. Rev. A*, vol. 73, 2006, Art. no. 013821.
- [4] S. Y. Lin, J. G. Fleming, E. Chow, J. Bur, K. K. Choi, and A. Goldberg, "Enhancement and suppression of thermal emission by a 3D photonic crystal," *Phys. Rev. B*, vol. 62, 2000, Art. no. R2243.
- [5] S. Y. Lin, J. Moreno, and J. G. Fleming, "Three-dimensional photonic crystal emitter for thermal photovoltaic power generation," *Appl. Phys. Lett.*, vol. 83, pp. 380–382, 2003.
- [6] S. Y. Lin, J. G. Fleming, and I. El-Kady, "Experimental observation of photonic-crystal emission near a photonic band-edge," *Appl. Phys. Lett.*, vol. 83, pp. 593–595, 2003.
- [7] M.-L. Hsieh, S. Y. Lin, J. Bur, and R. Shenoi, "Experimental observation of unusual thermal radiation from a 3D metallic photonic-crystal," *Nanotechnology*, vol. 26, 2015, Art. no. 234002.
- [8] The blackbody paint used in this experiment is a high temperature, $T = 300\text{--}1600$ K, ZYP Zirconium oxide paint. The material is electrically insulated and thermally conductive. Manufactured by ZYP Coatings, Tennessee, USA.
- [9] Z.-P. Yang, L. Ci, J. A. Bur, S.Y. Lin, and P. M. Ajayan, "Experimental Observation of an extremely dark material made by a low-density nanotube array," *Nano Lett.*, vol. 8, pp. 446–451, 2008.
- [10] Z.-P. Yang *et al.*, "Experimental observation of extremely weak optical scattering from an interlocking carbon nanotube array," *Appl. Opt.*, vol. 50, pp. 1850–1855, 2011.
- [11] Z. Han and A. Fina, "Thermal conductivity of carbon nano-tubes and their polymer nano composites: Review," *Prog. Polymer Sci.*, vol. 36, pp. 914–944, 2011.
- [12] K. M. Ho, C. T. Chan, C. M. Soukoulis, R. Biswas, and M. Sigalas, "Photonic band gaps in three dimensions: New layer-by-layer periodic structures," *Solid State Commun.*, vol. 89, pp. 413–416, 1994.
- [13] S. Y. Lin *et al.*, "A three-dimensional photonic crystal operating at infrared wavelengths," *Nature*, vol. 394, pp. 251–253, 1998.
- [14] J. G. Fleming, S. Y. Lin, I. El-Kady, R. Biswas, and K. M. Ho, "All-metallic three-dimensional photonic crystals with a large infrared bandgap," *Nature*, vol. 417, pp. 52–55, 2002.
- [15] E. F. Schubert, *Light-Emitting-Diodes*. Cambridge, U.K.: Univ. Cambridge Press, 2003, Ch. 8, pp. 171–172.
- [16] E. L. Dereziak and G. D. Boreman, *Infrared Detectors and Systems*, New York, NY, USA: Wiley, 1996, (For Planck's blackbody radiation formula, see Ch2. p.66 and p.70).
- [17] When the emitted photon energy ($\hbar\omega$) is much larger than the thermal energy ($\hbar\omega \gg k_b T$), the Bose-Einstein distribution function becomes approximately the Boltzmann distribution function, $1/(e^{\hbar\omega/k_b T} + 1) \cong e^{-\hbar\omega/k_b T}$. And, the ratio of the distribution function at two different temperatures (T_1 and T_2) becomes $\eta = (e^{-\hbar\omega/k_b T_2})/(e^{-\hbar\omega/k_b T_1})$. For the imaging study, when $\lambda = 1.7 \mu\text{m}$, $T_1 = 650$ K and $\eta = 3.7, 4.5,$ and 5.0 , we found $T_2 = 722, 735$ and 742 K, respectively. Again, the temperature in the W-PC region would have to be 72–92 K hotter than the VA-CNT region to account for the observed W-PC radiation enhancement. Please see Ref. [16] for Planck's blackbody radiation formula.
- [18] S. John and R. Wang, "Photonic band gap filament architectures for optimized incandescent lighting," *Phys. Rev. A*, vol. 78, 2008, Art. no. 43809.
- [19] M.-L. Hsieh, J. Bur, Q. Du, S. John, and S. Y. Lin, "Probing the intrinsic optical bloch-mode emission from a three-dimensional photonic crystal," *Nanotechnology*, vol. 27, 2016, Art. no. 415204.
- [20] B. N. J. Persson and A. Baratoff, "Theory of photon emission in electron tunneling to metallic particles," *Phys. Rev. Lett.*, vol. 68, pp. 3224–3227, 1992.
- [21] R. Aaswath, A. Marc, Z. Linxiao, E. Rephaeli, and S. Fan, "Theory "Passive radiative cooling below ambient air temperatures under direct sunlight," *Nature*, vol. 515, pp. 540–504, 2014.